The Fifth International Workshop on Micro and Nanotechnology for Power Generation and Energy Conversion Applications
PowerMEMS 2005
Nov. 28-30, 2005
Takeda Hall, The University of Tokyo, Tokyo, Japan

High-impulse, Low-power Digital Microthrusters Using Dissimilar Liquid Propellant Plug Pairs

Sang Wook Kim, Won Chul Lee, and Young-Ho Cho
Digital Nanolocomotion Center & Department of BioSystems
Korea Advanced Institute of Science and Technology
373-1 Guseong-dong, Yuseong-gu, Daejeon 305-701, Republic of Korea
Phn +82-42-869-4354; Fax +82-42-869-8690; E-mail: nanosys@kaist.ac.kr

ABSTRACT

A high-impulse, low-power microthruster has been developed using low-boiling-temperature liquid-propellant with high-viscous fluid-plug. The viscous friction of fluid-plug increases the blast pressure and the low-boiling-temperature liquid-propellant is intended to reduce input power consumption. The three-layer microthruster has been fabricated by surface micromachining as well as bulk micromachining in the size of 7±0.25mm×13±0.25mm× 1.5±0.25mm. At the continuous operation mode, the output impulse bit of 6.4×10^{-8} N·sec is obtained for the fabricated microthruster using perfluoro normal hexane (FC72) propellant and oil-plug.

Keywords: Microthruster, Microinjector, Digital Multiple Injection, Injection Propellant, and Plug pairs

1 INTRODUCTION

Recently, microinjectors [1~6] for the micropropulsion systems have been developed mainly for the attitude control of the microspacecraft, having the mass of 1~20kg [3]. The microinjector for the attitude control of the microspacecraft serves as the microthruster, generating the appropriate impulse.

Table 1 summarizes the microthruster requirements [3] for the attitude control of microspacecraft, having specific mass. As shown in Table 2, the impulse bit of the conventional liquid-propellant microthruster [1] is insufficient to satisfy the impulse requirement of Table 1. The impulse bit obtained from the solid-propellant microthruster [2] meets the impulse bit requirement of Table 1, but the operation is limited to the single shot.

In this paper, we present a microthruster using two dissimilar fluids, the low-boiling-temperature liquid-propellant and the high-viscous fluid-plug, to achieve a high-impulse, low-power, and continuous-shot micro-thruster.

2 WORKING PRINCIPLE

Figure 1 illustrates the working principle of the microthruster. In Fig. 1(a), the liquid-propellant is fed through the lower channel and the fluid-plug is fed through the upper channel. When the electrical input signal is supplied to the microheater, the liquid-propellant generates a bubble to build blast pressure. The viscous friction force of fluid-plug withholds high-pressure bubble to increase blasting impulse (Fig. 1(b)). After ejection, the liquid-propellant and the fluid-plug are fed by surface tension force, resulting in the initial state of Fig. 1(a).

Table 1. Specifications of the microthrusters for the attitude control of microspacecraft [3].

Mass of microspacecraft [kg]	Impulse bit [N·sec]	Thrust [mN]
20	1.3×10^{-5}	4.65
10	5×10^{-6}	1.75
1	7×10^{-7}	0.06

Table 2. Conventional MEMS-based microthrusters.

Propellant	Liquid [1]	Solid [2]
Input power	48 W	100 W
Impulse bit	6.6×10^{-9} N·sec	1×10^{-4} N·sec
Ejection mode	Continuous shot	Single shot

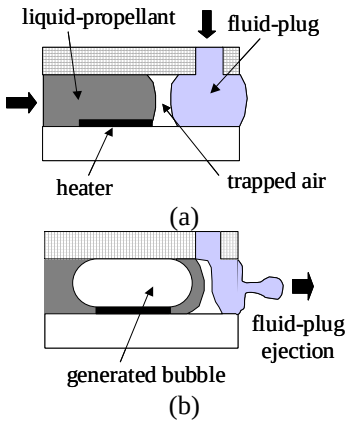

Figure 1. Working principle of the microthruster using low boiling temperature liquid-propellant with high-viscous fluid-plug; (a) the propellant and plug before ejection; (b) the propellant and plug at ejection.

3 FABRICATION PROCESS

Figure 2 shows the cross-sectional view of the present microthruster, composed of three layers shown in Fig. 3. Figure 3 shows the perspective view for the three-layer microthruster. The glass (bottom) layer contains a heater, electrical lines and channel for the liquid propellant. The silicon (middle) layer forms a channel for the fluid-plug and feed-holes for the liquid propellant, fluid-plug, and electrical interconnections, respectively. The polymer (top) layer contains three rectangular holes to provide the paths for the liquid propellant, fluid-plug, and electrical interconnections, respectively.

Figure 4 shows the fabrication process for the glass (bottom) layer, containing the electrical lines, the microheater and the channel for liquid propellant. Co-sputtering of 1000Å-thick TaAl is followed by the sputtering of 5000Å-thick Al layer (Fig. 4(a)). The Al and TaAl layers are etched in the Al etchant and the TaAl etchant, composed of HNO_3, H_2O and HF at the volumetric portion of 100:40:20. Additional photo-lithography and patterning of Al layer defines the microheater (Fig. 4(b)) in the size of 20μm-wide, 170μm-length, and 1000Å-thick. Finally, We use 40μm-thick PR (AZ9260) mold to form the liquid-propellant channel. Figure 5 shows the fabricated microheater, electrical lines and channel.

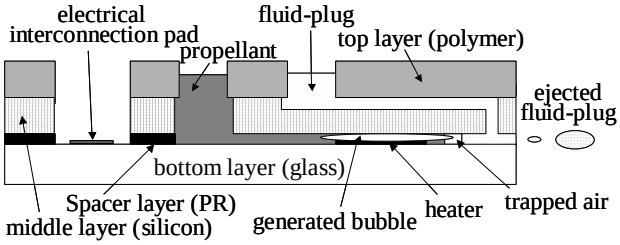

Figure 2. Cross-sectional view of the microthruster.

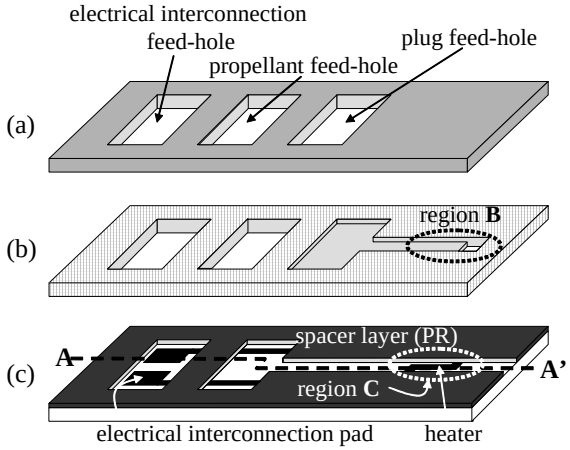

Figure 3. Perspective view of the microthruster layers: (a) top polymer layer; (b) middle silicon layer; (c) bottom glass layer.

On the silicon (middle) layer, the channel for the fluid-plug and the feed-holes are fabricated. The channel depth of 50μm is defined by ICP-RIE process using PR mask layer. The feed-holes for the liquid-propellant and electrical interconnections are formed by the second ICP-RIE process using the 5μm-thick PECVD oxide layer (TEOS).

After punching the feed-holes on the polymer (top) layer, the fabricated three layers have been bonded using 40μm-thick film adhesive (SHUR tape) to assemble the microthruster. Figure 6 shows the assembled microthruster in the size of 7±0.25mm×13±0.25mm× 1.5±0.25mm.

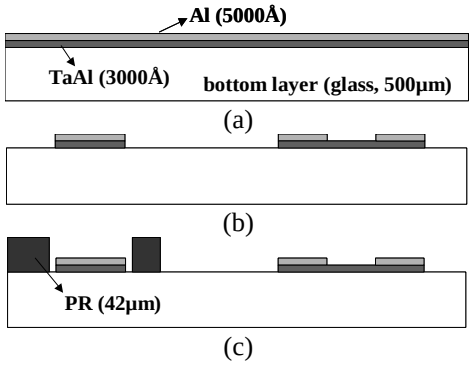

Figure 4. Fabrication process for the bottom layer of microthruster, showing the cross-section along A-A' in Fig. 3: (a) Al/TaAl sputtering; (b) Al/TaAl patterning; (c) thick PR molding.

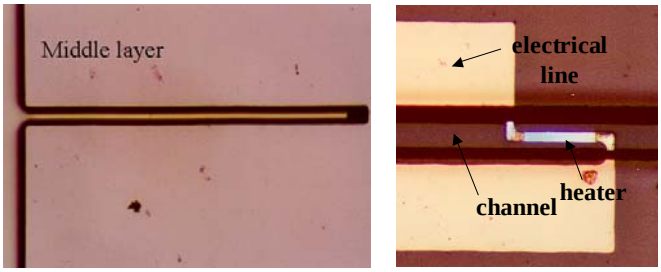

Figure 5. Photograph of the fabricated microchannel (b), showing the enlarged view of the region B in Fig.3(b), and heater (a), showing the top view of the region C in Fig.3(c).

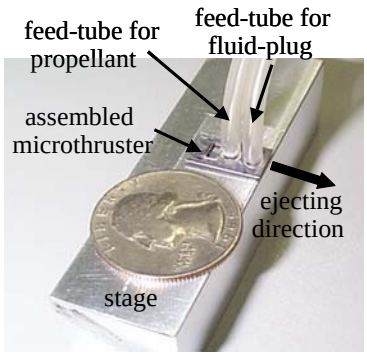

Figure 6. The fabricated microthruster, attached on the stage.

4 EXPERIMENTAL RESULTS

Figure 7 shows the schematic diagram for the experimental apparatus. We measure the ejection distance and the radius of ejected droplet, from which we extract the mass and initial ejection velocity of the droplet in order to estimate the blasting impulse. We also measure the turn-on pulse width, which is the minimum pulse width of the square wave signal required for the blasting.

Figure 8 shows the measured ejection distance and ejected droplet size for three different propellant and plug pairs such as water-water pair, perfluoro normal hexane (FC72, C_6F_6)-oil pair, and water-oil pair. In this work, we experimentally verify the viscous friction effect of the fluid-plug by comparing two different fluid-plug cases for the same liquid-propellant, and the boiling-temperature effect of the liquid-propellant by comparing two different liquid-propellant cases for the same fluid-plug. Table 3 shows the turn-on input energy versus impulse bit, estimated from the test using above three different kinds of the propellant and plug pairs.

First of all, we compare the impulse of the microthrusters using water-plug and oil-plug. In both cases, we use an identical geometry, the same propellant as water, and the same electrical input condition as 13V, 7Hz and 3msec pulse width square wave on the 420±0.5Ω resistance microheater.

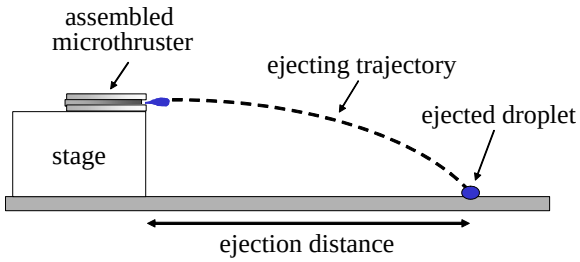

Figure 7. Illustration of the impulse measurement test.

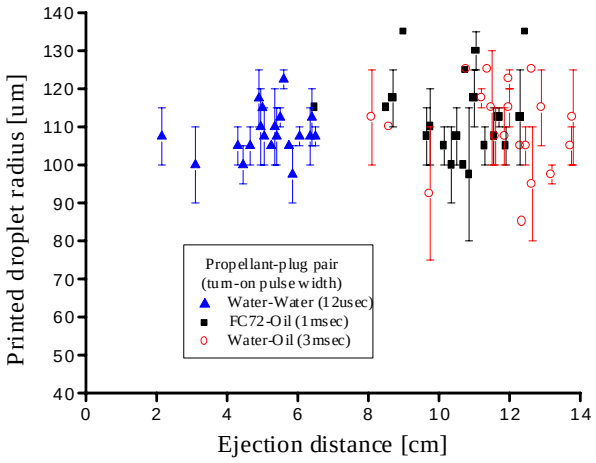

Figure 8. Measured ejection distances and printed radii of 20 ejected droplets, when 7Hz square wave voltage of 13V is supplied to the microheater of 420±0.5Ω.

Table 3. Measured turn-on input energy and output impulse for three different propellant-plug pairs.

Fluids Pair (Prop.- Plug)	Water-Water	Water-Oil	FC72-Oil
Turn-on pulse width	12±0.05* [μsec]	3±0.05* [msec]	1±0.05* [msec]
Droplet mass	5.34±0.9* [μg]	5.30±1.5* [μg]	5.78±1.7* [μg]
Droplet velocity	5.32±1.0* [m/s]	12.2±1.6* [m/s]	10.8±1.5* [m/s]
Impulse	2.86±0.81* [10^{-8} N·s]	6.40±1.89* [10^{-8} N·s]	6.21±2.13* [10^{-8} N·s]

*Standard deviation

Table 4. Measured input energy and out impulse for three different input pulse width using a water propellant and water plug pair.

Pulse width	12 μsec (turn-on)	1 msec	3 msec
Input energy	4.83±0.05* [μJ]	402±23* [μJ]	1210±28* [μJ]
Droplet mass	5.34±0.9* [μg]	4.88±0.9* [μg]	5.53±0.9* [μg]
Droplet velocity	5.32±1.1* [m/s]	5.24±1.1* [m/s]	5.69±0.8* [m/s]
Impulse	2.86±0.81* [10^{-8} N·s]	2.55±0.81* [10^{-8} N·s]	3.14±0.58* [10^{-8} N·s]

*Standard deviation

In the case of oil-plug, the impulse bit of 6.4×10^{-8}Ns is obtained, which is about twice larger than 3.1×10^{-8}Ns of the water-plug case due to higher viscous friction force of oil-plug. On the other hand, the turn-on pulse widths are measured as 3msec and 12μsec for the case of oil-plug and water-plug, respectively (Table 4). It illustrates that the viscous friction force of oil-plug suppresses the blasting pressure of water-propellant during the turn-on pulse width of 3ms, but the water-plug withholds the blasting pressure of water-propellant only for the turn-on pulse width of 12μs.

We also compare two different propellants such as water and FC72, whose boiling temperature is quite low as 59ºC, for the same oil-plug. As shown in Table 3, the impulse bit of above two case is almost same (6.4×10^{-8} Ns for the water-propellant and 6.2×10^{-8}Ns for the FC72-propellant, respectively), but in the case of water-propellant, three times larger input electrical energy is needed for making an impulse bit than that of the FC72-propellant case. It illustrates that FC72-propellant produces larger pressure expansion for the same input energy, because of its lower boiling temperature.

5 CONCLUSIONS

In this paper, we presented the high-impulse, low-power, continuous-shot microthruster using the high-viscous fluid-plug and low-boiling-temperature liquid-propellant for application to the attitude control of microspacecraft. In the experimental study, we fabricated microthruster and measured the ejection distance and ejected droplet size. From the measured values, we estimated the output impulse bit of the microthruster using two types of liquid-propellant, water and FC72, having different boiling-temperature and two types of fluid-plugs, water and oil, having different viscosity. In the case of oil-plug, the estimated impulse bit of 6.4×10^{-8} N·sec is twice greater than that of water-plug case. The input energy as 0.4±0.02mJ of FC72 propellant microthruster is reduced to one third of the water-propellant microthruster, producing an equivalent impulse bit.

On these experimental bases, we can conclude that present microthruster shows the potential for the low-power, high-impulse, and continuous-shot application, such as the attitude control of microsatellite, by separating two roles of the conventional propellant as the propellant and plug.

ACKNOWLEDGEMENT

This work has been supported by the National Creative Research Initiative Program of the Ministry of Science and Technology (MOST) under the project title of “Realization of Bio-Inspired Digital Nanoactuators.”

REFERENCES

[1] X. Ye, F. Tang, H. Ding and Z. Zhou, “A Vaporizing Water Micro-Thruster,” *Proceeding of IEEE Micro Electro Mechanical Systems Workshop*, Miyazaki, January 23-27, 2000, pp.74-79.

[2] D. H. Lewis, Jr., S. W. Janson, R. B. Cohen and E. K. Antonsson, “Digital Micropropulsion,” *Proceeding of IEEE Micro Electro Mechanical Systems Workshop*, Orland, Florida, USA, January 17-21, 1999, pp.517-522.

[3] J. Mueller, “Thruster Options for Microspacecraft: A Review and Evaluation of Existing Hardware and Emerging Technologies,” *AIAA*, Seattle, WA, USA, July, 1997, Paper 97-3058.

[4] A. Asai, T. HARA, and I.E. Franklin, “One-Dimensional Model of Bubble Growth and Liquid Flow in Bubble Jet Printers,” *Japanese Journal of Appl. Phys*., Vol. 26, No. 10, 1987, pp.1794-1801.

[5] S. Hirata, Y. Ishii, H. Matoba, and T. Inui, “An Inkjet Head Using Diaphragm Micro-actuator,” *Proceeding of IEEE Micro Electro Mechanical Systems Workshop*, San Diego, California, USA, February, 1996, pp. 418-423.

[6] X. Zhu, E. Tran, W. Wang, E.S. Kim, and S.Y. Lee, “Micromachined Acoustic-Wave Liquid Ejector,” *Tech. Dig. Solid-State Sensor and Actuator Workshop*, Hilton Head Island, SC, June 1996, pp.280-282.